FORWARD PRODUCTION OF CHARM STATES AND PROMPT SINGLE MUONS IN 350 GeV p–Fe INTERACTIONS

J.L. RITCHIE, A. BODEK [1], R. BREEDON [2], R.N. COLEMAN [3], W. MARSH [3], S.L. OLSEN, I.E. STOCKDALE
University of Rochester, Rochester, NY 14627, USA

B.C. BARISH, R.L. MESSNER [4], M.H. SHAEVITZ [5], E.J. SISKIND [6]
California Institute of Technology, Pasadena, CA 91125, USA

F.S. MERRITT
University of Chicago, Chicago, IL 60637, USA

H.E. FISK, Y. FUKUSHIMA [7], P.A. RAPIDIS
Fermilab, Batavia, IL 60510, USA

and

G. DONALDSON [8] and S.G. WOJCICKI
Stanford University, Stanford, CA 94305, USA

Received 10 March 1983

The forward production of charm states in 350 GeV p–Fe interactions has been studied via the production of prompt single muons with momentum $p \gtrsim 20$ GeV/c. The data indicate equal production of single μ^+ and μ^- events. The observed momentum distributions can be fit with the hypothesis that D mesons are produced with an invariant cross section proportional to $(1 - x_F)^{5.0 \pm 0.8} \exp[-(2 \pm 0.3)P_t]$ and do not favor a large diffractive cross section predicted by intrinsic charm models. Extrapolation of the distributions to $x_F = 0$ yields a total $D\bar{D}$ production cross section of 22.6 ± 2.1(±3.6)μb/nucleon on the assumption of a linear A dependence and 8% average semileptonic branching ratio of charm states.

We have investigated the forward production of charm states in hadronic collisions by measuring the production of prompt single muons. Prompt single muons originate from the semileptonic decays of charm states.

The density extrapolation technique was employed to separate prompt from non-prompt muons originating from the decays of long lived particles such as π's, K's and hyperons. Prompt dimuons were identified with a large acceptance muon identifier.

Data were taken with both a 350 GeV diffracted proton beam and a 278 GeV secondary π^- beam using the Fermilab N5 beam line in Laboratory E of the Neutrino Area. In this letter we report on the analysis of the 350 GeV proton data. The pion data are discussed in another letter [1]. The proton data are of interest as a test of various charm production models. For example, in QCD models [2,3] [‡1,2] the dominant

For footnotes see next page.

[1] Alfred P. Sloan Foundation Fellow.
[2] Present address: Rockefeller University, New York, NY 10021, USA.
[3] Present address: Fermilab, Batavia, IL 60510, USA.
[4] Present address: SLAC, Stanford, CA 94305, USA.
[5] Present address: Columbia University, New York, NY 10027, USA.
[6] Present address: NYCB Real-Time Computing Inc., 106 Rocky Point Gardens, Rocky Point, NY 11778, USA.
[7] Present address: Laboratory for High Energy Physics, Tsukuba-gun, Ibaraki-Ken 305, Japan.
[8] Present address: Watkins–Johnson Corp., 2525 N. First St., San Jose, CA 95131-1097, USA.

0 031-9163/83/0000–0000/$ 03.00

production mechanism for incident protons is gluon–gluon processes which yield very central D meson distributions. In intrinsic charm models [4–6] the production is peaked in the forward direction near $x_F = \frac{1}{2}$.

The detector consisted of an upstream beam line spectrometer that measured the momentum of each incoming hadron to ±0.4%, a target calorimeter which served as a variable density "beam dump", a muon identifier and an iron toroid spectrometer. Data were taken with incident beam intensities ranging between 1 to 2 ($\times 10^5$) protons per 1 second spill.

The target calorimeter consisted of 49 steel plates 0.75 m × 0.75 m in transverse dimensions with a scintillation counter on the downstream face of each plate. The plates were mounted independently on rails so that the spacing between the plates could be varied. Of the 2.4 m of steel comprising the target calorimeter, the density of the upstream most 1.7 meters was varied. Data were taken at three different effective densities, ρ, in the ratio $1 : \frac{2}{3} : \frac{1}{2}$, with the location of the mean interaction point kept fixed. The density was changed frequently such that there were three independent data sets for each density. The most compact density of the target was about $\frac{3}{4}$ that of steel.

In addition to serving as a variable density target, the calorimeter measured the total hadronic and electromagnetic energy of each interaction and the longitudinal location and development of the shower.

The muon identifier consisted of 42 3m × 3m scintillation counters and 21 3m × 3m wire spark chambers sandwiched periodically throughout the 4.5 m of steel. This device allowed identification of muons down to 5 GeV/c in momentum.

The toroid muon spectrometer consisted of 24 magnetized steel disks each 20 cm thick and 1.8 m in radius (with a 25 cm diameter hole) with scintillation counters every 20 cm of steel and spark chambers every 80 cm of steel. The toroids were displaced off-axis by 0.9 m to avoid a hole in the acceptance for forward going muons. The muon energy resolution was measured to the ±11% using beams of momentum tagged muons.

The trigger consisted of two components: an interacting hadron and a muon component, respectively. The hadron component required an interaction in the first 40 cm of steel (as indicated by a significant deposition of energy in the calorimeter), no counts in the halo counters and no additional beam particles within ±80 ns. This component was scaled to determine the incident flux of interacting hadrons. For monitoring purposes a random sample of interacting hadron triggers was recorded throughout the run. The interacting hadron component was put in coincidence with a muon that triggered the scintillation counters at the back of the toroid system. This corresponded to a minimum muon energy of about 20 GeV. Another trigger required a penetration of a muon in the muon identifier only, and corresponded to a minimum muon energy of 8 GeV. Half the data were taken at low intensity ($\simeq 10^4$/s) with the $p > 8$ GeV/c trigger. In this letter we report only on results obtained with the $p \gtrsim 20$ GeV/c trigger. The analysis of the $p > 8$ GeV/c data will be reported in a future publication.

In the off-line analysis each event was required to pass several selection criteria. These criteria were also applied to the random sample of hadron interactions in order to establish the effects of the cuts on the incident hadron flux. One important requirement was that of having only a *single* incoming hadron track with momentum within ±2.5% of the nominal beam momentum. This requirement and the hardware halo veto counters eliminated all upstream interactions. As a test, special runs were made with additional material upstream. The accepted event rates for such runs (which had 10 times the usual amount of material in *all* locations) remained unchanged.

The muon track was required to originate in the target calorimeter and be in the same RF bucket as the incoming hadron. Geometrical cuts were placed on the angle of the final state muon with respect to the direction of the incident hadron to ensure that the acceptance was independent of calorimeter configuration and small variations in beam conditions.

Events passing the selection criteria were placed in one of four categories: (1) a single μ^+ ($1\mu^+$), (2) a single μ^- ($1\mu^-$), (3) a dimuon with a triggering μ^+ $(2\mu)^+$, and (4) a dimuon with a triggering μ^- $(2\mu)^-$. Note that a dimuon event with opposite sign muons both of which trigger will fall into both (3) and (4) categories. The total trigger rates for these types of events

[‡1] A rough fit to the model of Carlson and Suaya yields a cross section $\propto \exp[-41/\sqrt{s}\,(\mathrm{GeV})]$ for p–p collisions.

[‡2] The model by Leveille predicts that in p–p collisions the cross section is $\propto s^{1.4}$ around $\sqrt{s} = 30$ GeV.

was plotted versus inverse density ($1/\rho$). The intercepts at $1/\rho = 0$ of the lines drawn through the $1\mu^+$ and $1\mu^-$ rates are the raw prompt $1\mu^+$ and $1\mu^-$ signals. Some single-muon events could be misclassified as dimuons because of a coincidental decay of an additional pion in the hadron shower. The probability of a decay yielding a muon with $p > 5$ GeV/c was determined, using the sample of random hadrons, to be 0.67% at the most compacted density for 350 GeV incident hadrons. The single-muon and dimuon rates were corrected for this small effect.

The largest background in the single-muon sample comes from highly asymmetric dimuon events in which one muon had momentum less than 5 GeV/c. This background was subtracted with the aid of a Monte Carlo calculation which reproduced the shapes and magnitude of the observed dimuon distributions. The Monte Carlo utilized measured [7] cross sections and distributions of the hadronic production of dimuons as a function of mass, Feynman-x, and p_T. It included production of dimuons by secondary particles in the hadron shower and the Bethe–Heitler conversion of photons from π^0 decays. In order to minimize the model dependence, the Monte Carlo was only used to determine the *fraction* of misidentified dimuon events (~15%) as a function of momentum. The *measured* rates of identified dimuon events multiplied by those fractions yielded the misidentified background. The observed raw rates for dimuon and single muon events as well as the calculated misidentified dimuon (fake 1μ) contributions are shown as a function of momentum in fig. 1.

Backgrounds arising from non-linearities [8] in the extrapolation procedure (e.g. from the finite thickness of the steel plates and the finite lifetime of hyperons, kaons and pions) were calculated to be 3% and 1.7% of the prompt signal for μ^+'s and μ^-'s respectively. Backgrounds from decays downstream of the variable density region (after 10 interaction lengths) were calculated using a shower Monte Carlo propagated through six shower generations and subtracted from the data. This correction was 3% and 1.6% of the prompt signal for μ^+'s and μ^-'s respectively.

The prompt single-muon momentum distributions (with all backgrounds removed) are shown in fig. 2. Also shown is the trigger efficiency which can be greater than 1 since it includes resolution smearing effects. The measured total prompt $1\mu^+$ and $1\mu^-$ rates are

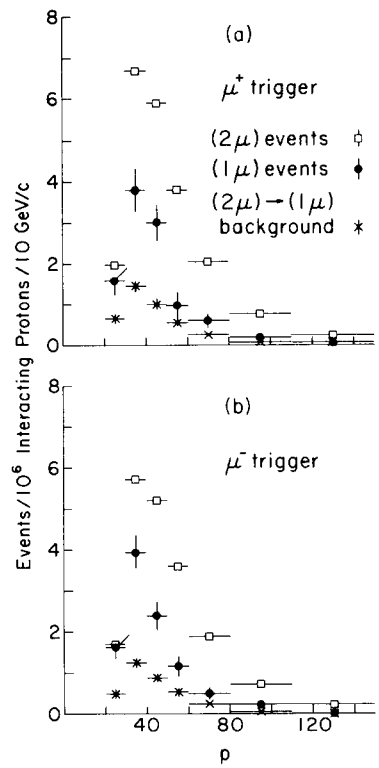

Fig. 1. Uncorrected momentum distributions for prompt 2μ (open square) and 1μ (solid dot) events. Also shown is the calculated contribution of the misidentified dimuons to the 1μ data sample (asterisk). (a) $1\mu^+$ and $(2\mu)^+$, (b) $1\mu^-$ and $(2\mu)^-$.

$(6.1 \pm 0.9) \times 10^{-6}$ and $(6.6 \pm 0.7) \times 10^{-6}$ per inelastic proton interaction, respectively. These errors are dominated by statistics but also include systematic errors in the background subtractions. These rates yield a raw prompt $1\mu^-/1\mu^+$ ratio of 1.08 ± 0.19. There is a small difference in trigger efficiency between μ^+ and μ^- events due to the fact that the geometrical acceptance of the muon spectrometer is not identical for positive and negative muons. The corrected number for the prompt $1\mu^-/1\mu^+$ ratio of 1.13 ± 0.20 is consistent with equal production of positive and negative single muons.

It is of interest to compare this ratio with the prompt $\bar{\nu}_\mu/\nu_\mu$ ratio measured in neutrino beam-dump experiments for prompt neutrinos with energies greater than 20 GeV. The ratios from the CERN beam-dump experiments BEBC (0.79 ± 0.62) and CHARM ($0.79^{+0.6}_{-0.5}$) are consistent with unity but have very

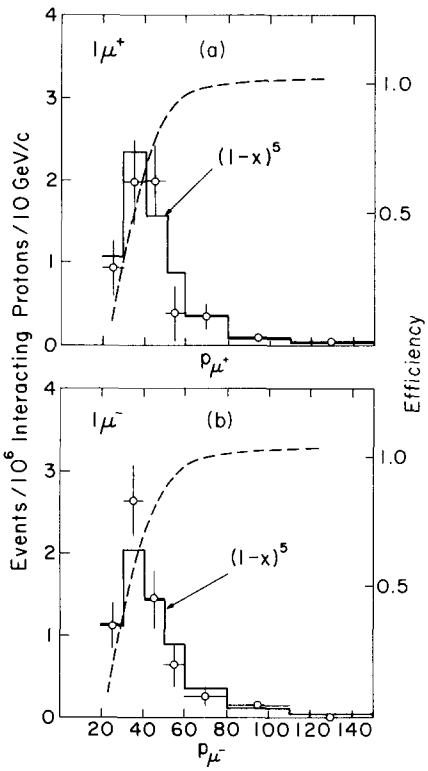

Fig. 2. Prompt single muon momentum distributions with all backgrounds removed (a) $1\mu^+$ and (b) $1\mu^-$. Also shown (solid line) are the predictions from a model in which D's are produced with a $(1 - |x|)^5$ distribution. The dashed line is the efficiency which can be greater than 1.0 since it includes resolution smearing effects.

large errors, while the CDHS experiment [9] quotes a ratio of $0.46^{+0.21}_{-0.16}$ which is not confirmed by our data. We note that the detectors of the CERN beam-dump experiments are located about a kilometer from the dump and subtend a very small solid angle [‡3]. Because of this geometrical factor and the energy dependence of the neutrino cross section those experiments are sensitive to neutrinos from the decay of charm states produced at very large Feynman-x ($x \approx 0.8$), in contrast to this experiment which is sensitive to D mesons with lower values of x ($x \gtrsim 0.1$). We have studied the $1\mu^-/1\mu^+$ ratio for $P_\mu > P_\mu^{\min}$ as a function of $P_\mu^{\min}$. Prompt single muons at large momenta originate from D mesons at large Feynman-x. The data are consistent with a ratio of unity at all values of $P_\mu^{\min}$ but the errors at high $P_\mu^{\min}$ are large.

The prompt single-muon distributions were compared to the prediction of a model in which the only source of prompt single muons are D mesons produced according to

Case (1):

$$E\, d^3\sigma_D/dp^3 \propto (1-x)^\alpha \exp(-bP_t)\,,$$

or:

Case (2):

$$E\, d^3\sigma_D/dp^3 \propto (1-x)^\alpha \exp(-b'm_t)\,,$$

with $m_t = (P_t^2 + m_D^2)^{1/2}$, x and P_t are the Feynman-x and transverse momentum of a D meson with mass m_D. We have assumed that the semileptonic decay modes of the D are $D \to K\mu\nu$ (60%) and $D \to K^*\mu\nu$ (40%). Single muons from the semileptonic decays of D's generated according to the model were propagated through the apparatus using a Monte Carlo program which included the effects of multiple scattering, dE/dx and resolution. The resulting "Monte Carlo tapes" were analyzed in the same way as the regular data. The model predictions included D production by secondary interactions in the calorimeter (which amounted to 15% of the primary contribution). In the calculation of the contribution of secondary interactions we have used the energy dependence of charm production from the QCD calculation of Carlson and Suaya [2]. The results that we quote for cross sections and distributions are for the *primary collisions* only.

Because of multiple Coulomb scattering in the calorimeter the data do not constrain the P_t fits very well. Separate fits to μ^+ and μ^- distributions yield consistent but poorly determined values of b and b'. A comparison of the model predictions with the P_t distributions of the combined μ^+ and μ^- prompt single-muon data yield $b = 2.0 \pm 0.3$ ($\chi^2 = 1.52$/degree of freedom) and $b' = 3.75 \pm 0.75$ ($\chi^2 = 1.53$/degree of freedom), where b and b' are in units of GeV^{-1}. A QCD calculation by Leveille [3] yields $b = 2.5$ and $b' = 3.45$. That model also predicts that the $\exp(-b'm_t)$ form should

[‡3] Preliminary data from the beam dump experiment at Fermilab (Experiment E613, FMOWW Collaboration), which has a similar acceptance to our $P_\mu \gtrsim 20$ GeV/c data, yield a ratio $\bar{\nu}_\mu/\nu_\mu = 0.65 \pm 0.30$, see ref. [10].

give a better description of D meson production especially at low P_t. The fits to our data indicate that D mesons are produced with a mean P_t of 0.92 ± 0.14 GeV/c and a mean P_t^2 of 1.2 ± 0.3 (GeV/c)^2. Our P_t distributions are consistent with results of the CERN NA16 experiment [11] using the high resolution bubble chamber LEBC which indicate a mean P_t^2 for D mesons produced in 360 GeV p–p collision of 0.9 ± 0.2 (GeV/c)^2.

The x acceptance of the detector is relatively insensitive to the shape of the P_t distributions. The extraction of the best fits to the D meson x distribution is done by comparing the model predictions to the momentum distributions of single-muon events in fig. 2. The best fit to the $1\mu^+$ data is obtained with the distribution

$$(1 - |x|)^{4.1 \pm {}^{1.7}_{1.1}} .$$

Extrapolation of this form to $x = 0$ yields a total cross section $\sigma_D(-1 < x < 1) = 17.8 \pm 2.6\ (\pm {}^{6.0}_{4.2})\ \mu$b/nucleon. The best fit to the $1\mu^-$ data is obtained with a distribution

$$(1 - |x|)^{5.4 \pm {}^{1.2}_{0.9}} ,$$

which yields a total cross section $\sigma_D(-1 < x < 1) = 25.9 \pm 2.7\ (\pm {}^{5.0}_{4.3})\ \mu$b/nucleon. A fit constraining both distributions to yield the same cross section and the same value of α yields the distribution

$$(1 - |x|)^{5.0 \pm 0.8} ,$$

and a total cross section $\sigma_{D\bar{D}} = 22.6 \pm 2.1\ (\pm 3.6)\ \mu$b/nucleon (see fig. 3). The cross sections were extracted assuming an average semileptonic branching ratio of 8% and a linear atomic weight dependence (A) for the cross section. The first error that is quoted includes the dominant statistical error and the systematic errors on background subtractions. The error in parenthesis is the systematic error in the extrapolation of the cross section to $x = 0$ from the uncertainty in the x dependence exponent α. Using the best fit to the x distribution we determine that 10.2% of the semileptonic decays of D's produced in the forward hemisphere are accepted by our trigger. The sensitivity of the extracted cross section to the power in $(1 - x)^\alpha$ is shown in fig. 3 along with the χ^2 values of the fits to the data. To the extent that $(1 - |x|)^\alpha$ is a proper description of charm production, the systematic error includes the model uncertainty.

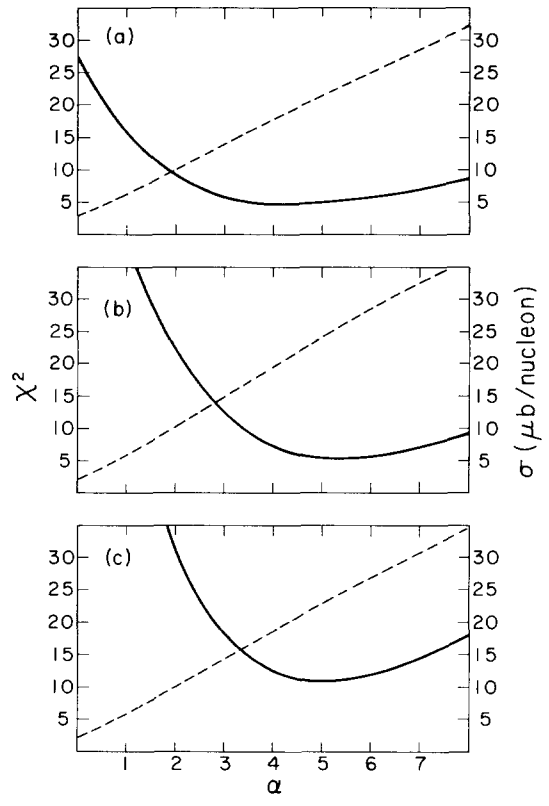

Fig. 3. The total charm production cross sections as a function of the exponent α in the $(1 - |x|)^\alpha$ distribution for D meson production (dashed line), and the χ^2 values of the fits to the data (solid line). (a) $1\mu^+$ data (D's) 6 degrees of freedom; (b) $1\mu^-$ data ($\bar{D}$'s), 6 degrees of freedom; (c) $1\mu^+$ and $1\mu^-$ data combined (D$\bar{D}$), 13 degrees of freedom. The cross sections are extracted assuming a linear A dependence and an 8% branching ratio.

The central-like x distribution suggests that gluon–gluon processes are important in charm production with incident protons at 350 GeV. For example, in the QCD calculation of ref. [3] the x distribution of the produced charm quarks has a dependence $(1 - |x|)^{5.1}$.

Preliminary results from the Fermilab neutrino beam-dump experiment [10] at 400 GeV indicate that $(1 - |x|)^5$ yields a somewhat better fit to their data than $(1 - |x|)^3$. Their D$\bar{D}$ cross section (extrapolated to $x = 0$ using a $(1 - |x|)^5$ form is 30 ± 6 μb, in good agreement with our data. Within QCD models [2,3] one expects a 10% to 20% increase in the cross section between 350 GeV and 400 GeV.

A comparison with charm cross sections extracted from the CERN neutrino beam-dump experiments [9, 12] is complicated by the fact that those experiments have smaller acceptance and typically assume a $(1-|x|)^3$ dependence of the cross section. In addition, some of them obtain a smaller charm cross section from the prompt electron neutrinos than from the prompt muon neutrinos. If we assume a $(1-|x|)^3$ dependence (not the best fit to our data) we obtain (see fig. 3) a cross section of 14.4 ± 1.2 μb/nucleon which is close to the cross section that those beam-dump experiments extract from their electron neutrino data. The Fermilab neutrino beam-dump experiment [10] obtains a cross section of 18 ± 4 μb, assuming a $(1-|x|)^3$ dependence.

The quoted systematic errors in the cross section do not include the uncertainty in the A dependence or in the semileptonic braching ratio. Some information on the A dependence and the average semileptonic branching ratio may be obtained by comparing our results to results obtained in 360 GeV p–p collisions in the LEBC hydrogen filled bubble chamber [11]. Their result of $\sigma_{\text{charm}} = 32^{+13}_{-9}$ is consistent with our result of 22.6 ± 2.1 (±3.6) where we have assumed a linear dependence and an 8% branching ratio. Note that our cross sections would be a factor of 3.8 larger if we assumed an $A^{2/3}$ dependence. The situation is not entirely clear because the LEBC data also imply $dN/dx \propto (1-|x|)^{1.8\pm0.8}$ for $x \geqslant 0$, which is flatter than what is indicated by our data. It is possible that the nuclear effects are a function of x and distort the x distribution in iron. For example, the A dependence for Λ and K production [13] is a function of x, and high x production is suppressed relative to low x production for nuclear targets. Our data with $p_\mu > 8$ GeV/c trigger (which has an acceptance for 80% of the forward hemisphere) will yield a more model independent total cross section, and could be directly compared to the LEBC results.

The central-like x distributions which are indicated by the data do not favor a large diffractive component predicted by intrinsic charm models. A 1% intrinsic charm ($c\bar{c}$) component in the nucleon wave function has been proposed by Brodsky et al. [4] to explain the large (300 μb to 1000 μb) forward charm production cross sections reported [14] at ISR energies ($\sqrt{s}$ = 60 GeV). A 1% intrinsic charm component implies a diffractive production cross section of 210 μb for 350 GeV incident protons, and Λ_c and $\bar{D}$ x distributions peaked near $x = 0.5$ (due to the fact that the massive charm quarks carry most of the proton momentum).

We have used the Brodsky x distributions for the Λ_c and $\bar{D}$ to obtain the spectra of the μ^+ [assuming 50% $\Lambda_c \to \Lambda^0\mu\nu$ and 50% $\Lambda_c \to \Lambda(1520)\mu\nu$] and μ^- (assuming 60% $\bar{D} \to K\mu\nu$ and 40% $\bar{D} \to K^*\mu\nu$) events. As was done for the central production fits, the contribution of diffractive production by secondary interactions was included. In order to obtain an upper limit on the contribution of the intrinsic charm process, we have assumed that *all* the prompt muons with $P_\mu > 50$ GeV/c are due to diffractive $\Lambda_c\bar{D}$ production. The fits to the data with $P_\mu > 50$ GeV/c yield

$$\sigma_{\Lambda_c}^{\text{intrinsic charm}} \leqslant 2.7 \pm 0.9\ \mu\text{b} \times A^{1.0}$$

$$\leqslant 10.3 \pm 3.2\ \mu\text{b} \times A^{2/3}\ ,$$

$$\sigma_{\bar{D}}^{\text{intrinsic charm}} \leqslant 1.3 \pm 0.3\ \mu\text{b} \times A^{1.0}$$

$$\leqslant 4.7 \pm 1.2\ \mu\text{b} \times A^{2/3}\ ,$$

where semileptonic branching ratios [15] of 4.5% ± 1.7% and 8% ± 1% were used for the Λ_c and $\bar{D}$ respectively. The quoted errors on limits represent the statistical errors from the fits. If we assume an $A^{2/3}$ dependence for diffractive production [4] then the 4.7 μb limit on the cross section implies [‡4] a limit on the intrinsic $c\bar{c}$ component of 0.022%. If we assume that the $\bar{D}$ state consists primarily of neutral D's (i.e. a 4% rather than an 8% branching ratio) then the limit becomes 0.044%. This limit is comparable to the limit of 0.012% extracted by this collaboration [16] from dimuon events with missing energy. A limit of 0.28% has been reported [17] by the European Muon Collaboration. Note that the above cross section limits are a factor of 3.8 smaller for the case of linear A dependence (as proposed by some authors [18]). The above limits apply only to the intrinsic charm process and a larger contribution from forward dissociation

[‡4] The relation between the intrinsic charm fraction P_c, and diffractive charm production at asymptotic energy depends on whether we take $P_c \equiv \sigma_{c\bar{c}}/\sigma_{\text{total}}$ as originally defined by Brodsky in ref. [4], and used in this analysis, $P_c \equiv \sigma_{c\bar{c}}/\sigma_{\text{elastic}}$ as proposed in ref. [5], or $P_c \equiv \sigma_{c\bar{c}}/\sigma_{\text{diffractive}}$ as proposed in ref. [6]. The above definitions differ by a factor of six.

processes with softer x distributions can be accommodated by the data.

In conclusion, the data on the forward production of prompt single muons in 350 GeV p–Fe interactions implies that D mesons are produced with an invariant cross section that has a $(1 - |x|)^{5.0 \pm 0.8}$ dependence. We extract a total charm production ($-1 < x < 1$) of 22.6 ± 2.1 (± 3.6) μb/nucleon assuming a linear A dependence of the cross section and an average semileptonic branching ratio of 8%. The data indicate that the contribution of the intrinsic charm process is very small.

We would like to thank Fermilab for its support. One of us (AB) would like to thank the Alfred P. Sloan Foundation for its support. This work was supported by the US Department of Energy and the National Science Foundation.

References

[1] J.L. Ritchie et al., Forward production of charm states and prompt single muons in 278 GeV π^-–Fe interactions, UR-829 (1983), unpublished.
[2] C.E. Carlson and R. Suaya, Phys. Lett. 81B (1979) 329.
[3] J.P. Leveille, A model of hadronic charm production, UM HE 82-20, unpublished.
[4] S.J. Brodsky et al., Phys. Lett. 93B (1980) 451; Phys. Rev. D23 (1981) 2745.
[5] G. Bertsch et al., Phys. Rev. Lett. 47 (1981) 297.
[6] D.P. Roy, Phys. Rev. Lett. 47 (1981) 312.
[7] K.J. Anderson et al., Phys. Rev. Lett. 37 (1976) 799, 803.
[8] A. Bodek, in: Proc. Particles and fields (Montreal, October 1979) ed. B. Margolis, p. 211.
[9] H. Abramowicz et al., Z. Phys. C13 (1982) 179.
[10] R.J. Loveless, in: Proc. Neutrino-82 Conf. (Balatonfured, Hungary) eds. A. Frenkel and L. Jenik, Vol. 1 (1982) p. 89.
[11] C.M. Fisher, in: Proc. 21st Intern. Conf. on High energy physics (Paris, July 1982) ed. P. Petiau and M. Proneuf, p. C2-146;
M. Aguilar-Benitez et al., Phys. Lett. 123B (1983) 103.
[12] P. Fritze et al., Phys. Lett. 96B (1980) 427;
M. Jonker et al., Phys. Lett. 96B (1980) 435.
[13] P. Skubic et al., Phys. Rev. D18 (1978) 3115.
[14] K.L. Gibboni et al., Phys. Lett. 85B (1979) 437;
W. Lockman et al., Phys. Lett. 85B (1979) 443;
D. Drijard et al., Phys. Lett. 81B (1979) 250;
M. Basile et al., Nuovo Cimento Lett. 30 (1981) 487.
[15] E. Vella et al., Phys. Rev. Lett. 48 (1982) 1515.
[16] A. Bodek et al., Phys. Lett. 113B (1982) 77.
[17] J.J. Aubert et al., Phys. Lett. 110B (1982) 73.
[18] V. Barger et al., Phys. Rev. D24 (1981) 1428; also DOE-ER/00881-215, (1981), unpublished.